Hybrid Digital-to-Analog Beamforming for Millimeter-Wave Systems with High User Density

Manish Nair, Qasim Zeeshan Ahmed and Huiling Zhu
School of Engineering and Digital Arts, University of Kent, Canterbury, CT2 7NT, United Kingdom.
Email: {mn307, q.ahmed and h.zhu}@kent.ac.uk

***Abstract*—Millimeter-wave (mm-Wave) systems with hybrid digital-to-analog beamforming (D-A BF) have the potential to fulfill 5G traffic demands. The capacity of mm-Wave systems is severely limited as each radio frequency (RF) transceiver chain in current base station (BS) architectures support only a particular user. In order to overcome this problem when high density of users are present, a new algorithm is proposed in this paper. This algorithm operates on the principle of selection combining (SC). This algorithm is compared with the state of the art hybrid D-A BF. The simulation results show that our proposed hybrid D-A BF using SC supports higher density of users per RF chain. Furthermore, our proposed algorithm achieves higher capacity than what is achieved by the current hybrid D-A BF systems.**

***Index Terms*—Hybrid beamforming, beamformer, precoder, selection combining, millimeter wave, 3D channel, multi user, interference, MIMO, mobile communications.**

I. Introduction

Millimeter-wave (mm-Wave) frequencies have the potential of addressing spectrum scarcity and capacity demands in current cellular bands [1]. Full scale implementation of digital systems by deploying a radio frequency (RF) transceiver chain per antenna element is impossible due to the constraints of cost, power consumption and signal processing complexity imposed by the RF front end and mixed signal components [2]. A practical solution will be to deploy a much smaller number of RF chains where each RF chain can support a large number of transmit (Tx) antenna elements, resulting in a hybrid digital-to analog (D-A BF) system. Therefore, hybrid D-A BF is one of the techniques of reducing the number of RF chains [3], [4], [5].

Hybrid D-A BF have been proposed in [6], [7], where the digital beamformer is equivalent to an identity matrix and the analog beamformer is equivalent to the hermitian of the channel. It is also shown that the overall capacity of the hybrid D-A BF system is limited as compared to the complete digital beamforming (D-BF) system because of the number of RF chains [6]. The major drawback in this type of hybrid D-A BF structure is that each RF chain can only support a particular user [6]. Therefore, the maximum number of users that can be supported by the BS cannot exceed the number of RF chains [6]. This will severely limit mobile capacity in future mm-Wave networks especially in high density user environments like train stations, stadiums or shopping malls. Therefore, new hybrid D-A BF schemes are required, which can support multiple users by employing a BS RF chain to achieve similar capacity gains as promised by the D-BF systems.

Superposition coding can be applied to the Tx symbols on a single stream to support multiple users through a RF chain. However, it cannot serve multiple users simultaneously as only a single 3 dimensional (3D) beam is formed [8]. In this paper, a new hybrid D-A BF algorithm for supporting multiple users is proposed. With this employed technique, each user will have its own separate 3D beam assisting in supporting multiple users simultaneously. This algorithm is implemented with the help of selection combining (SC). The SC algorithm is an analog beamforming (A-BF) technique which modifies the A-BF matrix by designating each and every antenna element to the selected users. The users and antennas are selected depending upon their instantaneous channel state information (CSI). However, the users experience multi-user interference (MUI) from the beamformed signals. Therefore, a low complexity MUI cancelling technique is proposed at the receiver (Rx). From our simulations, it can be observed that the proposed hybrid D-A BF using the SC algorithm achieves superior capacity gains to other hybrid D-A algorithms as proposed in [6], [7]. Our proposed hybrid D-A BF algorithm also accounts for the 3D mm-Wave channel for a multi-user system which is generated when planar antenna arrays are deployed [9], [10].

The reminder of this paper is organized as follows. In Section II, the system model is described. In Section III, we propose the hybrid D-A BF SC based algorithm. In Section IV, the simulation results for the mentioned BF techniques are discussed. Finally, the paper is concluded in Section V.

II. Description of the Hybrid D-A BF System

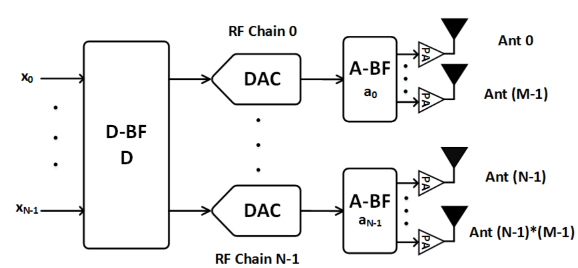

Figure 1. Hybrid BF Structure

The block diagram of the hybrid D-A BF system is shown in Fig. 1. This structure is preferred as it is common to the current cellular BS systems [6]. Each of the N RF chains is connected to a large-scale array of M identical antennas. The analysis is carried out considering a downlink scenario for the i-th RF chain supporting the k-th user. For the i-th RF chain the A-BF is performed over only M antennas by the analog beamformer $\boldsymbol{A}_i$. As the channel experiences L resolvable multipath [11], [12], [13], [14], [15], [16], the digital beamformer for the i-th chain is represented as $\boldsymbol{D}_i$ having dimensions $ML \times ML$. The complete digital beamformer $\boldsymbol{D}$ is given as:

$$\boldsymbol{D} = \text{diag}[\boldsymbol{D}_1, \boldsymbol{D}_2, \cdots, \boldsymbol{D}_N], \tag{1}$$

where $\boldsymbol{D}$ accounts for N-RF chains in the BS and is $NML \times NML$ dimensional.

A. 3D mm-Wave Channel Model

The 3D mm-Wave modified Saleh-Valenzuela (SV) channel impulse response (CIR) for the i-th RF chain and the m-th Tx antenna is given by [17], [18], [19]:

$$\begin{aligned} h^k_{i,m}(t) &= \sum_{v=0}^{V-1}\sum_{u=0}^{U-1} \alpha^k_{i,m,uv} h^k_{i,m,uv} \delta(t-\tau_v-\tau_{uv}) \\ &= \sum_{l=0}^{L-1} \alpha^k_{i,m,l} h^k_{i,m,l} \delta(t-l\tau), \end{aligned} \tag{2}$$

where $h^k_{i,m,l}$ is the k-th user CIR of l-th resolvable multi-path for the m-th Tx antenna of the i-th RF chain. V denotes the number of clusters, U the number of of resolvable multi-paths in one cluster, and $L = UV$ is the total number of resolvable multi-paths at the receiver. l is related to u and v by $l = vU+u$. In (2) $h^k_{i,m,uv} = |h^k_{i,m,uv}|e^{j\theta_{uv}}$ represents the fading gain of the u-th resolvable multi-path in the v-th cluster connecting the m-th antenna in the i-th RF chain to the k-th user. τ_v is the time-of-arrival (ToA) of the v-th cluster and $\tau_{uv} = u\tau$ denotes the ToA of the u-th resolvable multi-path in the v-th cluster. In our mm-Wave channel, it is assumed that the average power of a multi-path at a given delay is related to the power of the first resolvable multi-path of the first cluster through the following relationship [18], [19]:

$$P^k_{uv} = P^k_{00}\text{exp}\Big(-\frac{\tau_v}{\Psi}\Big)\text{exp}\Big(-\frac{\tau_{uv}}{\psi}\Big), \tag{3}$$

where $P^k_{uv} = P^k_l = |h^k_{i,m,uv}|^2$ represents the expected power of the u-th resolvable multi-path in the v-th cluster connecting the k-th user to the m-th antenna in the i-th RF BS chain. Ψ and ψ are the corresponding power delay constants of the cluster and the resolvable multi-path respectively. For the channel model to be generic, we assume that the delay spread, which is $(L-1)\tau$ of the mm-Wave channel spans $g \geq 1$ data bits, satisfying $(g-1)N_\tau \leq (L-1) \leq gN_\tau$, where N_τ is the number of time slots per symbol. Secondly, we assume that the L number of resolvable multipath components are randomly distributed, but they are the same over each symbol. Due to the wider bandwidth at mm-Wave, all the L multi-path components can be resolved at the Rx side [20], [21], and multi-path diversity will be exploited in the analog beamformer to significantly improve capacity in our proposed system.

The CIR experienced by the i-th RF chain and the k-th user is given as:

$$\boldsymbol{H}^k_i(t) = diag\left[\boldsymbol{H}^k_{i,0}(t), \boldsymbol{H}^k_{i,1}(t), \cdots, \boldsymbol{H}^k_{i,M-1}(t)\right], \tag{4}$$

where $\boldsymbol{H}^k_{i,m}(t)$ is the $L \times (2L-1)$ dimensional Block-Toeplitz temporal CIR convolution matrix associated with the i-th RF chain, m-th Tx antenna and the k-th user, given by (5) at the bottom of the page. Finally, $\boldsymbol{H}^k_i(t)$ will also be a temporal matrix be of dimension $ML \times M(2L-1)$.

The k-th user 3D BF gain $\alpha^k_{i,m,uv} = \alpha^k_{i,m,l}$ for every Tx antenna element of the i-th RF chain is given in (6). $F_{Rx,V}$ and $F_{Rx,H}$ are the Rx beam pattern for the vertical (V) and horizontal (H) polarizations, respectively. $F_{Tx,i,V}$ and $F_{Tx,i,H}$ are the Tx beam pattern for the i-th RF chain. $\phi^{VV}_l, \phi^{VH}_l, \phi^{HV}_l, \phi^{HH}_l$ are the initial random phases for vertical (VV), cross (VH, HV), and horizontal polarizations (HH) for the l resolvable multi-path. κ_m is the intra-cluster Rician K-factor associated with the m-th Tx antenna cluster [10]. ϑ_l and φ_l are the elevation and azimuth angle-of-arrival (AoA), respectively. Finally, $\theta_{l,m}$ and $\phi_{l,m}$ are the elevation and azimuth angle-of-departure (AoD) of the l-th resolvable multi-path and m-th Tx antenna in the i-th RF chain.

B. Received Symbols of Hybrid D-A BF

The L samples of received signal at the k-th user from the i-th RF chain is expressed as:

$$\boldsymbol{y}^k_i(t) = \boldsymbol{H}^k_i(t)\boldsymbol{A}_i(t)\boldsymbol{D}_i\boldsymbol{x}^k_i(t) + \boldsymbol{n}^k_i(t), \tag{7}$$

where

$$\boldsymbol{x}^k_i(t) = \left[\boldsymbol{x}^k_{i,0}(t), \boldsymbol{x}^k_{i,1}(t), \cdots, \boldsymbol{x}^k_{i,M-1}(t)\right]^T \tag{8}$$

are the $ML \times 1$ dimensional transmitted uncorrelated data symbols to the k-th user from the i-th RF chain. $\boldsymbol{x}^k_{i,m}(t) = [x^k_{i,m}(t), x^k_{i,m}(t-1), \cdots, x^k_{i,m}(t-L+1)]$ are the L symbol samples for all the l resolvable multi-paths, corresponding to the m-th Tx antenna in the i-th chain. BF design will be discussed in detail in the following section. $\boldsymbol{n}^k_i(t)$ is modelled as independent and identical distributed (iid) complex Gaussian random noise with zero mean and a variance of σ^2_i for the k-th user. The signal to noise ratio (SNR) of the i-th RF chain is denoted by γ_i and is given as [22]:

$$\gamma_i(\boldsymbol{D}_i, \boldsymbol{A}_i(t), \boldsymbol{H}^k_i(t)) = \gamma_0 \frac{|\boldsymbol{H}^k_i(t)\boldsymbol{A}_i(t)\boldsymbol{D}_i\boldsymbol{x}^k_i(t)|^2}{\sigma^2_i}, \tag{9}$$

where γ_0 is the average input SNR. Maximizing this SNR will lead to improved system capacity (in bit per second per Hz) for

$$\boldsymbol{H}^k_{i,m}(t) = \begin{bmatrix} h^k_{i,m,0}(t) & h^k_{i,m,1}(t) & \cdots & h^k_{i,m,L-1}(t) & 0 & \cdots & 0 \\ 0 & h^k_{i,m,0}(t-1) & h^k_{i,m,1}(t-1) & \cdots & h^k_{i,m,L-1}(t-1) & \cdots & 0 \\ \vdots & \ddots & \ddots & \ddots & \ddots & \vdots & \vdots \\ 0 & \cdots & 0 & h^k_{i,m,0}(t-L+1) & h^k_{i,m,1}(t-L+1) & \cdots & h^k_{i,m,L-1}(t-L+1) \end{bmatrix} \tag{5}$$

$$\alpha^k_{i,m,l} = \begin{bmatrix} F_{Rx,V}(\varphi_l, \vartheta_l) \\ F_{Rx,H}(\varphi_l, \vartheta_l) \end{bmatrix}^T \begin{bmatrix} e^{j\phi^{VV}_l} & \sqrt{\kappa^{-1}_m}e^{j\phi^{VH}_l} \\ \sqrt{\kappa^{-1}_m}e^{j\phi^{HV}_l} & e^{j\phi^{HH}_l} \end{bmatrix} \begin{bmatrix} F_{Tx,i,V}(\phi_{l,m}, \theta_{l,m}) \\ F_{Tx,i,H}(\phi_{l,m}, \theta_{l,m}) \end{bmatrix} \tag{6}$$

the k-th user associated with the i-th RF chain, and calculated as [22]:

$$C_i^k = \log_2[1 + \gamma_i(\boldsymbol{D}_i, \boldsymbol{A}_i(t), \boldsymbol{H}_i^k(t))] \tag{10}$$

Let us now proceed towards designing the BF matrices which maximize the SNR of the i-th RF chain.

III. Beamformer Design for Hybrid D-A BF

In this section, a type of hybrid D-A BF is considered for supporting a high density of users in mm-Wave systems. In the separate design of hybrid D-A BF as proposed in [6] - [7], the analog beamformer $\boldsymbol{A}_i = \boldsymbol{H}_i^H/||\boldsymbol{H}_i||_F$ is equal to the normalized hermitian of the channel. $||\boldsymbol{H}_i||_F$ is the Frobenius norm of the channel. The digital beamformer, $\boldsymbol{D}_i = \boldsymbol{I}$ is an identity matrix of size L. The BF matrix in this case is simply a matched filter (MF) as $\boldsymbol{A}_i\boldsymbol{D}_i = \boldsymbol{H}_i^H/||\boldsymbol{H}_i||_F$. However, high user density environment cannot be supported by this method. Therefore, the SC algorithm is proposed.

A. Hybrid D-A BF with Selection Combining (SC)

In SC algorithm, M antenna elements in the i-th RF chain have to be allocated to K users. K represents the total number of users in a high user density environment, that have to be supported by the i-th RF chain such that $K \leq M$. The allocation of antenna elements is based on the calculation of expected power of the 3D mm-Wave modified SV channel of every user. For the m-th antenna element in the i-th RF chain, the channel power associated with the k-th user is calculated as follows:

$$p_{i,m}^k = \sum_{l=0}^{L-1} |h_{i,m,l}^k|^2 \tag{11}$$

This process is repeated for all the K users for the m-th antenna element. The m-th antenna is then assigned to that user which has the maximum power:

$$k_m = \underset{k \in K}{\operatorname{argmax}} \left\{p_{i,m}^0, p_{i,m}^1, \cdots, p_{i,m}^{K-1}\right\}, \tag{12}$$

where argmax calculates the maximum value. This process is repeated M times until all the M antennas are allocated to the S users where $S \leq K$. The remaining $(K - S)$ users are not supported.

It is clear that SC algorithm allocates non-contiguous antenna elements to the respective users. Therefore, the users will experience MUI from the beamformed signals generated from antenna elements that are allocated to other users. Interference from the undesired beamformed signals can be eliminated at every user by a set of receive BF weights. It is assumed that the SC antenna allocation information is available at the receiver. For example, consider a scenario in which the number of antenna elements in the i-th RF chain is $M = 4$, the total number of single antenna users to be supported by this i-th RF chain is $S = 3$, and where the SC antenna allocation for the i-th RF chain that follows the pattern as shown in Fig. 2. In this scenario, antenna m_0 is allocated to user s_0; m_1 and m_3 to s_2; and m_2 to s_1. As shown in the figure, A-BF $\boldsymbol{A}_i^{SC}(t)$ is performed over each of the M antennas, where as MUI suppression is implemented by

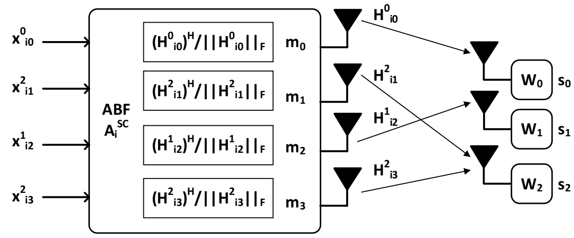

Figure 2. SC Antenna Allocation for the i-th RF chain

the weights $\boldsymbol{w}_s$ at the s-th user. The A-BF matrix $\boldsymbol{A}_i^{SC}(t)$, as depicted in Fig. 2 is given by:

$$\boldsymbol{A}_i^{SC}(t) = diag \begin{bmatrix} \boldsymbol{H}_{i,0}^{0\;H}(t)/||\boldsymbol{H}_{i,0}^0||_F \\ \boldsymbol{H}_{i,1}^{2\;H}(t)/||\boldsymbol{H}_{i,1}^2||_F \\ \boldsymbol{H}_{i,2}^{1\;H}(t)/||\boldsymbol{H}_{i,2}^1||_F \\ \boldsymbol{H}_{i,3}^{2\;H}(t)/||\boldsymbol{H}_{i,3}^2||_F \end{bmatrix}, \tag{13}$$

where $\boldsymbol{H}_{i,m}^s(t)$ represents the CIR from the m-th Tx antenna to the s-th user as was defined in (5). Now let us examine the case of user s_2. The received signal at s_2 can be represented as:

$$\begin{aligned} \boldsymbol{y}_i^{s_2}(t) &= \boldsymbol{w}_2\boldsymbol{H}_{i,1}^2(t)\boldsymbol{A}_i^{SC}(t)\boldsymbol{x}_i(t) + \boldsymbol{w}_2\boldsymbol{H}_{i,3}^2(t)\boldsymbol{A}_i^{SC}(t)\boldsymbol{x}_i(t) \\ &+ \underbrace{\boldsymbol{w}_2\boldsymbol{H}_{i,0}^2(t)\boldsymbol{A}_i^{SC}(t)\boldsymbol{x}_i(t)}_{\text{Interference from user } s_0} + \underbrace{\boldsymbol{w}_2\boldsymbol{H}_{i,2}^2(t)\boldsymbol{A}_i^{SC}(t)\boldsymbol{x}_i(t)}_{\text{Interference from user } s_1} \\ &+ \boldsymbol{w}_2\boldsymbol{n}_{i,2}(t) \end{aligned} \tag{14}$$

In (14), $\boldsymbol{x}_i(t) = [\boldsymbol{x}_{i,0}^0(t), \boldsymbol{x}_{i,1}^2(t), \boldsymbol{x}_{i,2}^1(t), \boldsymbol{x}_{i,3}^2(t)]^T$ is the $ML \times 1$ symbol vector for the i-th chain, where $\boldsymbol{x}_{i,m}^s(t) = [x_{i,m}^s(t), x_{i,m}^s(t-1), \cdots, x_{i,m}^s(t-L+1)]$ is the $L \times 1$ symbol vector assigned to the m-th antenna that is allocated to the s-th user by the SC algorithm. $\boldsymbol{n}_{i,2}(t)$ is the iid complex Gaussian random noise for the user s_2 with a variance of $\sigma_{i,2}^2$. $\{\boldsymbol{H}_{i,m}^2(t)\boldsymbol{A}_i^{SC}(t)\}$ is the $ML \times ML$ signal received at s_2 after analog preprocessing at the Tx and channel conditioning given by (15) at the top of the following page. In (15) $h_{i,m,l}^2(t)$ is the l-th resolvable multi-path at time instant t as defined previously. The $1 \times ML$ Rx-BF selection weights $\boldsymbol{w}_2 = [\boldsymbol{0}, \boldsymbol{1}, \boldsymbol{0}, \boldsymbol{1}]$, where the $\boldsymbol{0}$'s and $\boldsymbol{1}$'s are L dimensional, operating on $\{\boldsymbol{H}_{i,m}^2(t)\boldsymbol{A}_i^{SC}(t)\}$, will cancel the MUI from the unwanted beamformed signals that are generated by antenna elements allocated to the other users by the SC algorithm. It can be observed that the pattern of zeros follow the MUI's from the respective antenna elements which need to be eliminated. $\boldsymbol{D}_i$ is identity similar to [6], [7]. The weights for the other users for mitigating MUI can be similarly derived as $\boldsymbol{w}_0 = [\boldsymbol{1}, \boldsymbol{0}, \boldsymbol{0}, \boldsymbol{0}]$ and $\boldsymbol{w}_1 = [\boldsymbol{0}, \boldsymbol{0}, \boldsymbol{1}, \boldsymbol{0}]$ respectively, and can be extended for any SC antenna allocation. In this way, the receiver complexity can be reduced significantly because processing is moved to the Tx side. To satisfy the total power constraint the signal power of the i-th RF chain is:

$$\frac{1}{M}\sum_{m=0}^{M-1}\sum_{s=0}^{S-1} p_{i,m}^s \leq \sigma_i^2\gamma_i \tag{16}$$

Finally, the SNR for the i-th RF chain and the s-th user for the

$$
\boldsymbol{H}_{i,m}^2(t)\boldsymbol{A}_i^{SC}(t) = diag\begin{bmatrix} \boldsymbol{H}_{i,0}^2(t)\boldsymbol{H}_{i,0}^0(t)^H/||\boldsymbol{H}_{i,0}^0||_F \\ \boldsymbol{H}_{i,1}^2(t)\boldsymbol{H}_{i,1}^2(t)^H/||\boldsymbol{H}_{i,1}^2||_F \\ \boldsymbol{H}_{i,2}^2(t)\boldsymbol{H}_{i,2}^1(t)^H/||\boldsymbol{H}_{i,2}^1||_F \\ \boldsymbol{H}_{i,3}^2(t)\boldsymbol{H}_{i,3}^2(t)^H/||\boldsymbol{H}_{i,3}^2||_F \end{bmatrix} = diag\begin{bmatrix} \sum_{l=0}^{L-1}|h_{i,0,l}^2(t)h_{i,0,l}^0(t)|/||\boldsymbol{H}_{i,0}^0||_F \\ \sum_{l=0}^{L-1}|h_{i,0,l}^2(t-1)h_{i,0,l}^0(t-1)|/||\boldsymbol{H}_{i,0}^0||_F \\ \vdots \\ \sum_{l=0}^{L-1}|h_{i,0,l}^2(t-L+1)h_{i,0,l}^0(t-L+1)|/||\boldsymbol{H}_{i,0}^0||_F \\ \sum_{l=0}^{L-1}|h_{i,1,l}^2(t)|^2/||\boldsymbol{H}_{i,1}^2||_F \\ \sum_{l=0}^{L-1}|h_{i,1,l}^2(t-1)|^2/||\boldsymbol{H}_{i,1}^2||_F \\ \vdots \\ \sum_{l=0}^{L-1}|h_{i,1,l}^2(t-L+1)|^2/||\boldsymbol{H}_{i,1}^2||_F \\ \sum_{l=0}^{L-1}|h_{i,2,l}^2(t)h_{i,2,l}^1(t)|/||\boldsymbol{H}_{i,2}^1||_F \\ \sum_{l=0}^{L-1}|h_{i,2,l}^2(t-1)h_{i,2,l}^1(t-1)|/||\boldsymbol{H}_{i,2}^1||_F \\ \vdots \\ \sum_{l=0}^{L-1}|h_{i,2,l}^2(t-L+1)h_{i,2,l}^1(t-L+1)|/||\boldsymbol{H}_{i,2}^1||_F \\ \sum_{l=0}^{L-1}|h_{i,3,l}^2(t)|^2/||\boldsymbol{H}_{i,3}^2||_F \\ \sum_{l=0}^{L-1}|h_{i,3,l}^2(t-1)|^2/||\boldsymbol{H}_{i,3}^2||_F \\ \vdots \\ \sum_{l=0}^{L-1}|h_{i,3,l}^2(t-L+1)|^2/||\boldsymbol{H}_{i,3}^2||_F \end{bmatrix} \tag{15}
$$

SC algorithm is calculated as follows [22]:

$$
\gamma_i(\boldsymbol{w}_s, \boldsymbol{D}_i, \boldsymbol{A}_i^{SC}(t), \boldsymbol{H}_i^s(t)) = \frac{M_s\gamma_0}{M}|(\sigma_{i,s}^2\boldsymbol{w}_s^H)^{-1}\boldsymbol{w}_s^H\boldsymbol{H}_i^s(t) \times \boldsymbol{A}_i^{SC}(t)\boldsymbol{D}_i\boldsymbol{D}_i^H\boldsymbol{A}_i^{SC^H}(t) \times \boldsymbol{H}_i^{s^H}(t)\boldsymbol{w}_s|, \tag{17}
$$

where M_s is the number of antennas allocated to the s-th user and $\sigma_{i,s}^2$ is the corresponding iid noise variance.

IV. Simulation Results

Table I
3D mm-Wave Modified SV Channel Parameters [10]

Description	Unit	Value
Inter-cluster inter-arrival rate	$1/\mathrm{ns}$	0.21
Intra-cluster inter-arrival rate	$1/\mathrm{ns}$	0.77
Inter-cluster decay factor	ns	4.19
Intra-cluster decay factor	ns	1.07
Small-scale fading RMS	dB	1.26
Inter-cluster Rician K-factor	dB	-10
Intra-cluster Rician K-factor	dB	-10

In this section, beam pattern and the capacity performance of two different kinds of hybrid D-A BF algorithms are investigated. SC based hybrid D-A BF is compared with the separate hybrid D-A BF proposed in [6], [7]. The parameters for generating the 3D mm-Wave modified SV channel model are mentioned in Table-I [10]. Perfect channel knowledge or CSI [23], [24], [25], [26], [27], [28], [29], [30], [31], [32] is assumed between the Tx antennas and Rx antenna. Two different environments are considered in our simulations. In the first environment perfect line-of-sight (LoS) is available. While, in the second environment, multipath are present, and the number of resolvable multipath is assumed to be 15. A uniform planar array of $M = 16 \times 16$ antennas is considered.

Fig. 3 indicates that by using the SC algorithm to design the hybrid D-A BF system, the capacity increases when the number of users per RF chain increases. This is because with a larger number of users, the number of resolvable multipath in the mm-Wave channel increases which are combined using A-BF to improve the SNR at the respective users. In this way, multi-path diversity has been exploited in our mm-Wave system. This is observed in the curves with $K = 8$ users and $L = 15$ resolvable multipath per Tx antenna cluster attaining the upper bound as compared to the single user case with $L = 15$ resolvable multipath. $K = 8$ users per RF chain in a BS is chosen to represent a high user density scenario in mm-Wave systems. However, capacity gains from multipath diversity will be offset by the power constraint in the i-th RF chain, and it will tend to saturate. From this figure, it can also be observed that the SC algorithm outperforms the separate hybrid D-A BF design. Substantial gains in terms of performance are achieved by using our algorithm.

Fig. 4 in the following page plots the beam patterns generated by the $M = 16 \times 16$ planar BS antenna array in the i-th RF chain. Fig. 4a shows the pattern for a single user, with separate hybrid D-A BF design as in [6], [7]. Fig. 4b shows the pattern generated for a second and a third user in addition to the first user for the same RF chain using the SC algorithm.

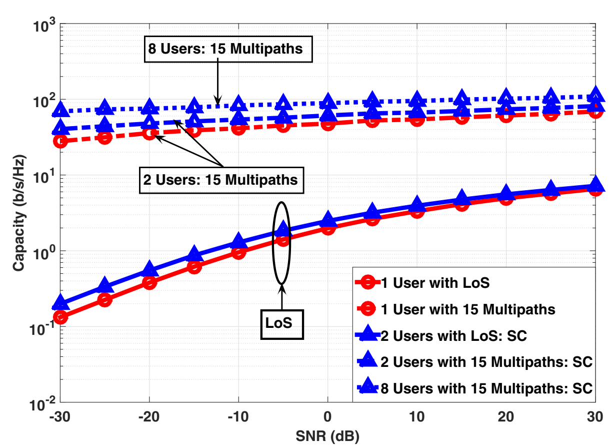

Figure 3. Capacity of the proposed hybrid D-A BF systems as a function of SNR. Results are reported for a downlink mmWave system with $M = 16 \times 16$ BS antennas from SNR of -30dB to 30dB. The simulated environment includes both a single LoS channel and $L = 15$ multi-path.

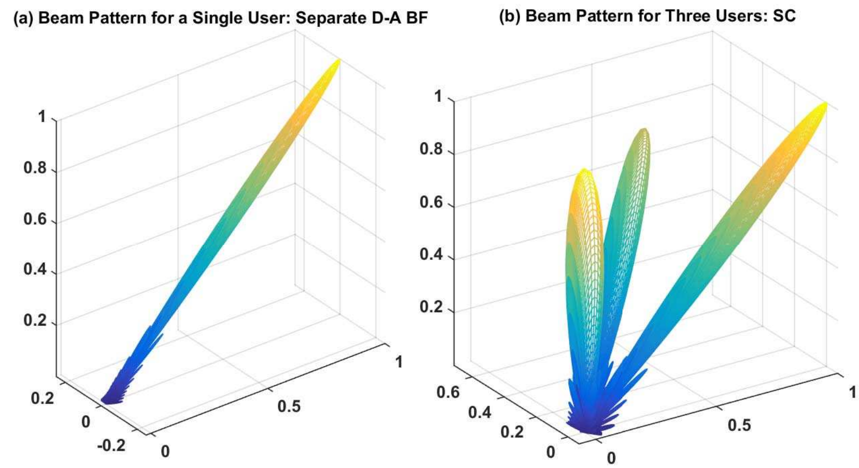

Figure 4. Normalized beam pattern for $M = 16 \times 16$ planar array using separate hybrid D-A BF design and SC. (a) Beam pattern of the original user in Separate Hybrid D-A BF Design. The angular location of the user is at $\theta = 0°$ from the y-z plane $\phi = 30°$ from the x-z plane, and, (b) Hybrid D-A BF design using SC. The combined beam patterns for the 3 users. The angular location of the 1-st user is unchanged, where as that of the 2-nd user is $\theta = 45°$ from the y-z plane $\phi = 45°$ from the x-z plane, and that of the 3-rd user is $\theta = 0°$ from the y-z plane $\phi = 90°$ from the x-z plane. The beam directivity is reduced in SC.

It can be observed from Fig. 4b that while SC achieves user separation, the directivity of the beams are reduced. This is because the number of antenna elements allocated per user is reduced, and at the same time, selection combining does not design the D-BF matrix, keeping it as identity as in the case of separate hybrid D-A BF design. In our simulations, the number of BS antenna array elements is chosen considering the processing and bandwidth limitations of the massive multiple-input multiple-output (MIMO) architectures.

V. Conclusion

In this paper, a new algorithm which operates on the principle of SC has been proposed for hybrid D-A BF based mm-Wave system. From our based algorithm, it is possible to support more than a single user per RF chain. This algorithm has a significant impact when higher density of users are present and the particular RF chain had to support multiple users. From our simulations, it has been seen that our proposed hybrid D-A BF using SC achieves higher capacity as compared to the known hybrid D-A BF and supports higher density of users per RF chain.

Acknowledgement

This work has received funding from the EU's Horizon 2020 Programme under Grant Agreement No. 643297 (RAPID 5G).

References

[1] S. Sun, T. Rappaport, R. Heath, A. Nix, and S. Rangan, "MIMO for Millimeter-Wave Wireless Communications: Beamforming, Spatial multiplexing, or Both," *IEEE Communications Magazine*, vol. 52, no. 12, pp. 110–121, December 2014.

[2] A. Alkhateeb, J. Mo, N. Gonzalez-Prelcic, and R. Heath, "MIMO Precoding and Combining Solutions for Millimeter-Wave Systems," *IEEE Communications Magazine*, vol. 52, no. 12, pp. 122–131, December 2014.

[3] M. Crocco and A. Trucco, "Design of Superdirective Planar Arrays With Sparse Aperiodic Layouts for Processing Broadband Signals via 3-D Beamforming," *IEEE/ACM Transactions on Audio, Speech, and Language Processing*, vol. 22, no. 4, pp. 800–815, April 2014.

[4] T. E. Bogale and L. B. Le, "Beamforming for multiuser massive mimo systems: Digital versus hybrid analog-digital," in *2014 IEEE Global Communications Conference*, Dec 2014, pp. 4066–4071.

[5] O. Alluhaibi, Q. Z. Ahmed, C. Pan, and H. Zhu, "Capacity Maximisation for Hybrid Digital-to-Analog Beamforming mm-Wave Systems," *to appear in IEEE Global Communications Conference (GLOBECOM"16)*, Dec. 2016.

[6] S. Han, C.-L. I, Z. Xu, and C. Rowell, "Large-Scale Antenna Systems with Hybrid Analog and Digital Beamforming for Millimeter Wave 5G," *IEEE Communications Magazine*, vol. 53, no. 1, pp. 186–194, January 2015.

[7] W. Roh, J.-Y. Seol, J. Park, B. Lee, J. Lee, Y. Kim, J. Cho, K. Cheun, and F. Aryanfar, "Millimeter-Wave Beamforming as an Enabling Technology for 5G Cellular Communications: Theoretical Feasibility and Prototype Results," *IEEE Communications Magazine*, vol. 52, no. 2, pp. 106–113, February 2014.

[8] H. T. Do and S. Y. Chung, "Linear beamforming and superposition coding with common information for the gaussian mimo broadcast channel," *IEEE Transactions on Communications*, vol. 57, no. 8, pp. 2484–2494, Aug 2009.

[9] A. Alkhateeb, O. El Ayach, G. Leus, and R. Heath, "Hybrid Precoding for Millimeter Wave Cellular Systems with Partial Channel Knowledge," in *2013 Information Theory and Applications Workshop (ITA)*, Feb 2013, pp. 1–5.

[10] H. Xu, V. Kukshya, and T. Rappaport, "Spatial and Temporal Characteristics of 60-GHz Indoor Channels," *IEEE Journal on Selected Areas in Communications*, vol. 20, no. 3, pp. 620–630, Apr 2002.

[11] H. Zhu and J. Wang, "Chunk-based resource allocation in ofdma systems - part i: chunk allocation," *IEEE Transactions on Communications*, vol. 57, no. 9, pp. 2734–2744, September 2009.

[12] ——, "Chunk-based resource allocation in ofdma systems - part ii: Joint chunk, power and bit allocation," *IEEE Transactions on Communications*, vol. 60, no. 2, pp. 499–509, February 2012.

[13] H. Zhu, "Radio resource allocation for ofdma systems in high speed environments," *IEEE Journal on Selected Areas in Communications*, vol. 30, no. 4, pp. 748–759, May 2012.

[14] H. Zhu and J. Wang, "Performance analysis of chunk-based resource allocation in multi-cell ofdma systems," *IEEE Journal on Selected Areas in Communications*, vol. 32, no. 2, pp. 367–375, February 2014.

[15] Y. Zhou, H. Liu, Z. Pan, L. Tian, J. Shi, and G. Yang, "Two-stage cooperative multicast transmission with optimized power consumption and guaranteed coverage," *IEEE Journal on Selected Areas in Communications*, vol. 32, no. 2, pp. 274–284, February 2014.

[16] A. Mahbas, "Double spectrum small cell (dssc) for discovering inter-frequency small cell in hetnet," in *2015 IEEE International Conference on Communications (ICC)*, June 2015, pp. 3454–3459.

[17] O. El Ayach, S. Rajagopal, S. Abu-Surra, Z. Pi, and R. Heath, "Spatially

Sparse Precoding in Millimeter Wave MIMO Systems," *IEEE Transactions on Wireless Communications*, vol. 13, no. 3, pp. 1499–1513, March 2014.
[18] Q. Z. Ahmed, K. H. Park, M. S. Alouini, and S. Assa, "Compression and combining based on channel shortening and reduced-rank techniques for cooperative wireless sensor networks," *IEEE Transactions on Vehicular Technology*, vol. 63, no. 1, pp. 72–81, Jan 2014.
[19] Q. Z. Ahmed and L. L. Yang, "Reduced-rank adaptive multiuser detection in hybrid direct-sequence time-hopping ultrawide bandwidth systems," *IEEE Transactions on Wireless Communications*, vol. 9, no. 1, pp. 156–167, January 2010.
[20] A. Alkhateeb and R. W. Heath, "Frequency selective hybrid precoding for limited feedback millimeter wave systems," *IEEE Transactions on Communications*, vol. PP, no. 99, pp. 1–1, 2016.
[21] C. Rusu, R. Mndez-Rial, N. Gonzlez-Prelcic, and R. W. Heath, "Low complexity hybrid sparse precoding and combining in millimeter wave mimo systems," in *2015 IEEE International Conference on Communications (ICC)*, June 2015, pp. 1340–1345.
[22] A. Goldsmith, S. A. Jafar, N. Jindal, and S. Vishwanath, "Capacity limits of mimo channels," *IEEE Journal on Selected Areas in Communications*, vol. 21, no. 5, pp. 684–702, June 2003.
[23] H. Zhu, "Performance comparison between distributed antenna and microcellular systems," *IEEE Journal on Selected Areas in Communications*, vol. 29, no. 6, pp. 1151–1163, June 2011.
[24] J. Wang, H. Zhu, and N. J. Gomes, "Distributed antenna systems for mobile communications in high speed trains," *IEEE Journal on Selected Areas in Communications*, vol. 30, no. 4, pp. 675–683, May 2012.
[25] H. Zhu and J. Wang, "Radio resource allocation in multiuser distributed antenna systems," *IEEE Journal on Selected Areas in Communications*, vol. 31, no. 10, pp. 2058–2066, October 2013.
[26] H. Osman, H. Zhu, D. Toumpakaris, and J. Wang, "Achievable rate evaluation of in-building distributed antenna systems," *IEEE Transactions on Wireless Communications*, vol. 12, no. 7, pp. 3510–3521, July 2013.
[27] T. Alade, H. Zhu, and J. Wang, "Uplink spectral efficiency analysis of in-building distributed antenna systems," *IEEE Transactions on Wireless Communications*, vol. 14, no. 7, pp. 4063–4074, July 2015.
[28] H. Zhu, S. Karachontzitis, and D. Toumpakaris, "Low-complexity resource allocation and its application to distributed antenna systems [coordinated and distributed mimo]," *IEEE Wireless Communications*, vol. 17, no. 3, pp. 44–50, June 2010.
[29] H. Zhu, "On frequency reuse in cooperative distributed antenna systems," *IEEE Communications Magazine*, vol. 50, no. 4, pp. 85–89, April 2012.
[30] H. Zhu, B. Xia, and Z. Tan, "Performance analysis of alamouti transmit diversity with qam in imperfect channel estimation," *IEEE Journal on Selected Areas in Communications*, vol. 29, no. 6, pp. 1242–1248, June 2011.
[31] V. Garcia, Y. Zhou, and J. Shi, "Coordinated multipoint transmission in dense cellular networks with user-centric adaptive clustering," *IEEE Transactions on Wireless Communications*, vol. 13, no. 8, pp. 4297–4308, Aug 2014.
[32] A. Mahbas, H. Zhu, and J. Wang, "Unsynchronized small cells with a dynamic tdd system in a two-tier hetnet," in *2016 IEEE 83rd Vehicular Technology Conference (VTC Spring)*, May 2016, pp. 1–6.